Dentate Gyrus NMDA Receptors Mediate Rapid Pattern Separation in the Hippocampal Network

Thomas J. McHugh, *et al.*

Science **317**, 94 (2007);
DOI: 10.1126/science.1140263

The eumetazoan progenitor was more than just a collection of genes. How did these genes function together within the ancestor? Unfortunately, we cannot read from the genome the nature of its gene- and protein-regulatory interactions and networks. This is particularly vexing as it is becoming clear—especially given the apparent universality of the eumetazoan toolkit—that gene regulatory changes can also play a central role in generating novelties, allowing co-option of ancestral genes and networks to new functions (*49*). Of particular interest are the processes that give rise to body axes, germ layers, and differentiated cell types such as nerve and muscle, as well as the mechanisms that maintain these cells and their interactions through the growth and repair of the organism. *Nematostella* and its genome provide a platform for testing hypotheses about the nature of ancestral eumetazoan pathways and interactions, with the use of the basic principle of evolutionary developmental biology: Processes that are conserved between living species were likely functional in their common ancestor.

References and Notes

1. E. Haeckel, *Generelle Morphologie der Organismen*, vols. 1 and 2 (Georg Reimer, Berlin, 1866).
2. C. Nielsen, in *Animal Evolution* (Oxford Univ. Press, Oxford, ed. 2, 2001), pp. 51–58.
3. J. W. Valentine, in *On the Origin of Phyla* (Univ. Chicago Press, Chicago, 2004), pp. 153–196.
4. G. M. Rubin *et al.*, *Science* **287**, 2204 (2000).
5. G. Ruvkun, O. Hobert, *Science* **282**, 2033 (1998).
6. C. I. Bargmann, *Science* **282**, 2028 (1998).
7. P. Dehal *et al.*, *Science* **298**, 2157 (2002).
8. Sea Urchin Genome Sequencing Consortium *et al.*, *Science* **314**, 941 (2006).
9. D. Bridge, C. W. Cunningham, B. Schierwater, R. DeSalle, L. W. Buss, *Proc. Natl. Acad. Sci. U.S.A.* **89**, 8750 (1992).
10. G. Narbonne, *Annu. Rev. Earth Planet. Sci.* **33**, 421 (2005).
11. S. Conway Morris, *Philos. Trans. R. Soc. London Ser. B* **361**, 1069 (2006).
12. C. Hand, K. Uhlinger, *Biol. Bull.* **182**, 169 (1992).
13. J. A. Darling *et al.*, *Bioessays* **27**, 211 (2005).
14. C. Hand, K. Uhlinger, *Estuaries* **17**, 501 (1994).
15. J. H. Fritzenwanker, U. Technau, *Dev. Genes Evol.* **212**, 99 (2002).
16. R. E. Steele, *Dev. Biol.* **248**, 199 (2002).
17. R. D. Kortschak, G. Samuel, R. Saint, D. J. Miller, *Curr. Biol.* **13**, 2190 (2003).
18. U. Technau *et al.*, *Trends Genet.* **21**, 633 (2005).
19. D. J. Miller, E. E. Ball, U. Technau, *Trends Genet.* **21**, 536 (2005).
20. B. Galliot, *Curr. Opin. Genet. Dev.* **10**, 629 (2000).
21. K. Seipel *et al.*, *Dev. Dyn.* **231**, 303 (2004).
22. S. Reber-Muller *et al.*, *Int. J. Dev. Biol.* **50**, 377 (2006).
23. M. Q. Martindale, K. Pang, J. R. Finnerty, *Development* **131**, 2463 (2004).
24. J. R. Finnerty, D. Paulson, P. Burton, K. Pang, M. Q. Martindale, *Evol. Dev.* **5**, 331 (2003).
25. J. H. Fritzenwanker, M. Saina, U. Technau, *Dev. Biol.* **275**, 389 (2004).
26. C. B. Scholz, U. Technau, *Dev. Genes Evol.* **212**, 563 (2003).
27. A. H. Wikramanayake *et al.*, *Nature* **426**, 446 (2003).
28. C. G. Extavour, K. Pang, D. Q. Matus, M. Q. Martindale, *Evol. Dev.* **7**, 201 (2005).
29. M. Q. Martindale, J. R. Finnerty, J. Q. Henry, *Mol. Phylogenet. Evol.* **24**, 358 (2002).
30. F. Raible *et al.*, *Science* **310**, 1325 (2005).
31. J. L. Weber, E. W. Myers, *Genome Res.* **7**, 401 (1997).
32. Materials and methods, as well as additional text, are available as supporting material on *Science* Online.
33. R. L. Tatusov, E. V. Koonin, D. J. Lipman, *Science* **278**, 631 (1997).
34. A. Adoutte *et al.*, *Proc. Natl. Acad. Sci. U.S.A.* **97**, 4453 (2000).
35. Y. I. Wolf, I. B. Rogozin, E. V. Koonin, *Genome Res.* **14**, 29 (2004).
36. F. D. Ciccarelli *et al.*, *Science* **311**, 1283 (2006).
37. J. Y. Chen *et al.*, *Dev. Biol.* **248**, 182 (2002).
38. K. J. Peterson *et al.*, *Proc. Natl. Acad. Sci. U.S.A.* **101**, 6536 (2004).
39. E. J. Douzery, E. A. Snell, E. Bapteste, F. Delsuc, H. Philippe, *Proc. Natl. Acad. Sci. U.S.A.* **101**, 15386 (2004).
40. J. C. Sullivan, A. M. Reitzel, J. R. Finnerty, *Genome Informatics* **17**, 219 (2006).
41. I. B. Rogozin, Y. I. Wolf, A. V. Sorokin, B. G. Mirkin, E. V. Koonin, *Curr. Biol.* **13**, 1512 (2003).
42. J. S. Conery, M. Lynch, *Pac. Symp. Biocomput.* **2001**, 167 (2001).
43. J. H. Postlethwait *et al.*, *Genome Res.* **10**, 1890 (2000).
44. O. Jaillon *et al.*, *Nature* **431**, 946 (2004).
45. The Honeybee Genome Sequencing Consortium, *Nature* **443**, 931 (2006).
46. G. Bourque, E. M. Zdobnov, P. Bork, P. A. Pevzner, G. Tesler, *Genome Res.* **15**, 98 (2005).
47. L. G. Lundin, D. Larhammar, F. Hallbook, *J. Struct. Funct. Genomics* **3**, 53 (2003).
48. K. J. Meaburn, T. Misteli, *Nature* **445**, 379 (2007).
49. M. Levine, R. Tjian, *Nature* **424**, 147 (2003).
50. J. R. Finnerty, K. Pang, P. Burton, D. Paulson, M. Q. Martindale, *Science* **304**, 1335 (2004).
51. K. Kamm, B. Schierwater, W. Jakob, S. L. Dellaporta, D. J. Miller, *Curr. Biol.* **16**, 920 (2006).
52. J. F. Ryan *et al.*, *Genome Biol.* **7**, R64 (2006).
53. D. Chourrout *et al.*, *Nature* **442**, 684 (2006).
54. K. Kamm, B. Schierwater, *J. Exp. Zoolog. B. Mol. Dev. Evol.* (Jul 12, 2006).
55. J. R. Finnerty, M. Q. Martindale, *Evol. Dev.* **1**, 16 (1999).
56. F. Delsuc, S. F. Vizcaino, E. J. Douzery, *BMC Evol. Biol.* **4**, 11 (2004).
57. M. Long, E. Betran, K. Thornton, W. Wang, *Nat. Rev. Genet.* **4**, 865 (2003).
58. A. Kusserow *et al.*, *Nature* **433**, 156 (2005).
59. K. Seipel, V. Schmid, *Int. J. Dev. Biol.* **50**, 589 (2006).
60. K. Seipel, V. Schmid, *Dev. Biol.* **282**, 14 (2005).
61. C. A. Byrum, M. Q. Martindale, in *Gastrulation: From Cells to Embryos*, C. D. Stern, Ed. (Cold Spring Harbor Laboratory Press, Cold Spring Harbor, NY, 2004), pp. 33–50.
62. F. G. Giancotti, E. Ruoslahti, *Science* **285**, 1028 (1999).
63. S. Tyler, *Int. Comp. Biol.* **43**, 55 (2003).
64. A. Pires-daSilva, R. J. Sommer, *Nat. Rev. Genet.* **4**, 39 (2003).
65. D. Q. Matus *et al.*, *Proc. Natl. Acad. Sci. U.S.A.* **103**, 11195 (2006).
66. D. Q. Matus, G. H. Thomsen, M. Q. Martindale, *Curr. Biol.* **16**, 499 (2006).
67. P. N. Lee, K. Pang, D. Q. Matus, M. Q. Martindale, *Semin. Cell Dev. Biol.* **17**, 157 (2006).
68. F. Rentzsch *et al.*, *Dev. Biol.* **296**, 375 (2006).
69. M. Miljkovic-Licina, D. Gauchat, B. Galliot, *Biosystems* **76**, 75 (2004).
70. D. Gauchat *et al.*, *Dev. Biol.* **275**, 104 (2004).
71. F. Jacob, *Science* **196**, 1161 (1977).

72. This work was performed under the auspices of the U.S. Department of Energy's Office of Science, Biological and Environmental Research Program, and by the University of California, Lawrence Livermore National Laboratory under contract no. W-7405-Eng-48, Lawrence Berkeley National Laboratory under contract no. DE-AC02-05CH11231, and Los Alamos National Laboratory under contract no. DE-AC02-06NA25396 and was supported by NIH–National Heart, Lung, and Blood Institute grant THL007279F. Genetic Information Research Institute is under the NIH grant 5 P41 LM006252-09. D.S.R., M.S., and W.D. gratefully acknowledge the support of the Gordon and Betty Moore Foundation. We thank H. Marlow, D. Matus, K. Pang, P. Lee, and C. Magie for contributions to fig. S1; and E. Begovic, E. Edsinger-Gonzales, D. Goodstein, M. Carpenter, C. David, M. Levine, J. Gerhart, and J. Valentine for useful conversations.

Supporting Online Material

www.sciencemag.org/cgi/content/full/317/5834/86/DC1
Materials and Methods
SOM Text
Figs. S1.1 to S7.4
Tables S1.1 to S8.1
References

21 December 2006; accepted 4 June 2007
10.1126/science.1139158

Dentate Gyrus NMDA Receptors Mediate Rapid Pattern Separation in the Hippocampal Network

Thomas J. McHugh,[1,2]* Matthew W. Jones,[1]*† Jennifer J. Quinn,[3]‡ Nina Balthasar,[4]† Roberto Coppari,[4]§ Joel K. Elmquist,[4]§ Bradford B. Lowell,[4] Michael S. Fanselow,[3] Matthew A. Wilson,[1] Susumu Tonegawa[1,2]‖

Forming distinct representations of multiple contexts, places, and episodes is a crucial function of the hippocampus. The dentate gyrus subregion has been suggested to fulfill this role. We have tested this hypothesis by generating and analyzing a mouse strain that lacks the gene encoding the essential subunit of the *N*-methyl-D-aspartate (NMDA) receptor NR1, specifically in dentate gyrus granule cells. The mutant mice performed normally in contextual fear conditioning, but were impaired in the ability to distinguish two similar contexts. A significant reduction in the context-specific modulation of firing rate was observed in the CA3 pyramidal cells when the mutant mice were transferred from one context to another. These results provide evidence that NMDA receptors in the granule cells of the dentate gyrus play a crucial role in the process of pattern separation.

The hippocampus is crucial for the formation of memories of facts and episodes (*1*–*4*). To allow similar episodes to be distinguished, it must rapidly form distinct representations of the temporal and spatial relationships comprising events (pattern separation), and because specific episodes are rarely replicated in full, the hippocampus must also be capable of

using partial cues to retrieve previously stored representations (pattern completion). Specific hippocampal subregions and circuits have been suggested to subserve these mnemonic requirements: the feedforward pathway from the entorhinal cortex (EC) to the dentate gyrus (DG) and on to CA3 for pattern separation, and the recurrent and highly plastic connections in CA3 for pattern completion (*5*–*8*). Recently, targeted genetic manipulations provided strong evidence for the role of plastic CA3 recurrent synapses in pattern completion (*9*, *10*). However, evidence supporting the hypothesis of pattern separation at the behavioral level has been scant and limited to interpretation of impairments observed in rodents with DG lesions (*11*, *12*)

The activity of hippocampal neurons ("place cells") depends on an animal's location in the environment (*13*), and many studies suggest that ensemble place cell activity encodes memory traces (*14*–*18*). Recent studies have directly investigated whether physiological correlates of behavioral pattern separation can be detected in the hippocampal circuits by means of the place cell recording technique (*19*–*26*). One finding particularly relevant to our current study (*20*) is that exposure of rats to two similar but distinct contexts generates place cell firing rates in the two contexts that overlap significantly less in CA3 than in CA1. Although consistent with the hypothesis (*6*–*8*) that the DG helps separate the overlapping representation patterns as they reach the CA3 region, this study did not directly test the role of the EC→DG→CA3 circuit in behavioral and physiological separation, nor propose a mechanism for the process.

Generating dentate gyrus granule cell–specific NMDA receptor knockout mice. In one of several mouse lines using a proopiomelanocortin (POMC)–bacterial artificial chromosome to drive expression of the Cre recombinase (*27*), crossing with lacZ reporter mice [Rosa26 (*28*)] revealed robust Cre-loxP recombination in the DG granule cell (GC) layer throughout the dorsal/ventral axis (Fig. 1, A to D), with sparser recombination in the arcuate nucleus of the hypothalamus, the lateral habenular nucleus, and a small number of scattered cortical and midbrain cells. Immunofluorescence studies with antibodies specific for β-galactosidase (a Cre-loxP recombination marker), NeuN (a neuronal marker), S100β (a glial cell marker), and glutamic acid decarboxylase (GAD-67, an interneuron marker) indicated that the Cre-loxP recombination is confined to GCs in the DG of the hippocampus (Fig. 1, E to K). Cre-loxP recombination in the DG GC layer begins between postnatal weeks 2 to 3 and remains spatially restricted until at least 24 weeks of age (fig. S1). It is known that DG GCs can arise via adult neurogenesis. Cre-loxP recombination is detected in newly born neurons that had reached the GC layer (Fig. 1, L to N).

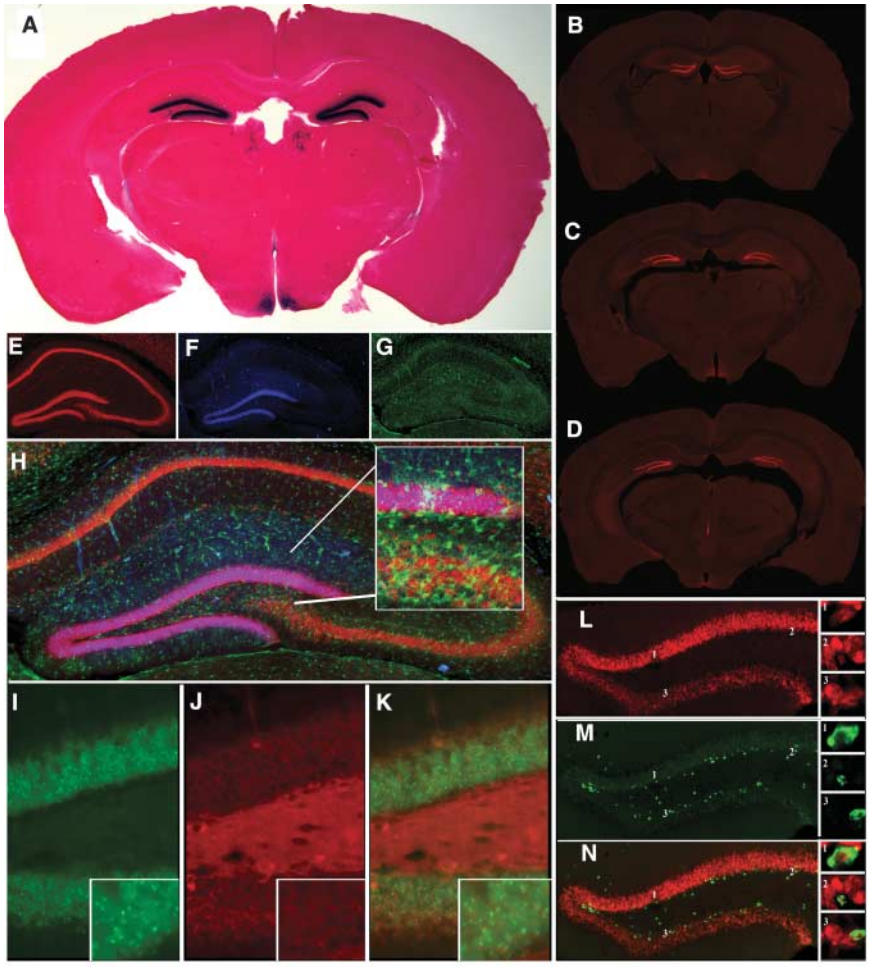

Fig. 1. Basic features of POMC-Cre transgenic mice. (**A**) Image (1× magnification) of β-galactosidase (β-Gal) expression in a 12-week-old POMC-Cre/ROSA26 double-transgenic mouse stained with X-Gal and nuclear fast red. (**B** to **D**) Anti–β-Gal immunohistochemical (1×, images visualized with Cy3, red) staining showing expression in a 16-week-old POMC-Cre/ROSA26 double-transgenic mouse in three coronal sections taken along the rostro-caudal axis of the forebrain. (**E** to **K**) Immunofluorescence staining of coronal sections of a 20-week-old POMC-Cre/ROSA26 double-transgenic mouse. Single staining with (E) anti-NeuN (neuronal marker; AlexaFlour 555, red, 4×), (F) anti–β-Gal (marker of Cre recombination; aminomethylcoumarin, blue, 4×), and (G) anti-s100β (glial cell marker; fluorescein isothiocyanate, green, 4×). (H) A 4× merge of (E), (F), and (G) indicating that the Cre-loxP recombination is restricted to the neurons in the DG. Inset is a 20× image of the DG. (I to K) Single staining with (I) an anti–β-Gal (AlexaFlour488, green, 20×) and (J) anti-GAD67 (marker of inhibitory neurons; Cy3, red, 20×). (K) A merge of (I) and (J), indicating no recombination in GAD-67–positive inhibitory neurons. In the bottom right corner of each figure is a magnified image of several cells in the upper blade of the DG showing the separation of the green and red signals. (**L** to **N**) After injection of bromodeoxyuridine (BrdU) into a 12-week-old male POMC-Cre/ROSA26 double-transgenic mouse, brain sections were imaged by confocal microscopy. To the right of each 10× image are three single cells imaged at 63× at the positions in the 10× image labeled with the corresponding number. Single staining with (L) anti–β-Gal (Cy3, red) and (M) anti-BrdU (marker of newly born cells; AlexaFlour488, green). (N) The overlap of the green and red signal in the cells imaged indicates that recombination occurs in newly born neurons after they reach the GC layer.

[1]The Picower Institute for Learning and Memory, RIKEN–MIT Neuroscience Research Center, Department of Biology and Department of Brain and Cognitive Sciences, Massachusetts Institute of Technology, Cambridge, MA 02139, USA. [2]Howard Hughes Medical Institute, Massachusetts Institute of Technology, Cambridge, MA 02139, USA. [3]Department of Psychology, University of California–Los Angeles, Los Angeles, CA 90095, USA. [4]Division of Endocrinology, Harvard Medical School, Beth Israel Deaconess Medical Center, Boston, MA 02215, USA.

*These authors contributed equally to this work.
†Present address: Department of Physiology, University of Bristol, Bristol BS8 1TD, UK.
‡Present address: Division of Molecular Psychiatry, Yale University, New Haven, CT 06508, USA.
§Present address: Center for Hypothalamic Research, University of Texas Southwestern Medical Center, Dallas, TX 75390, USA.
‖To whom correspondence should be addressed. E-mail: tonegawa@mit.edu

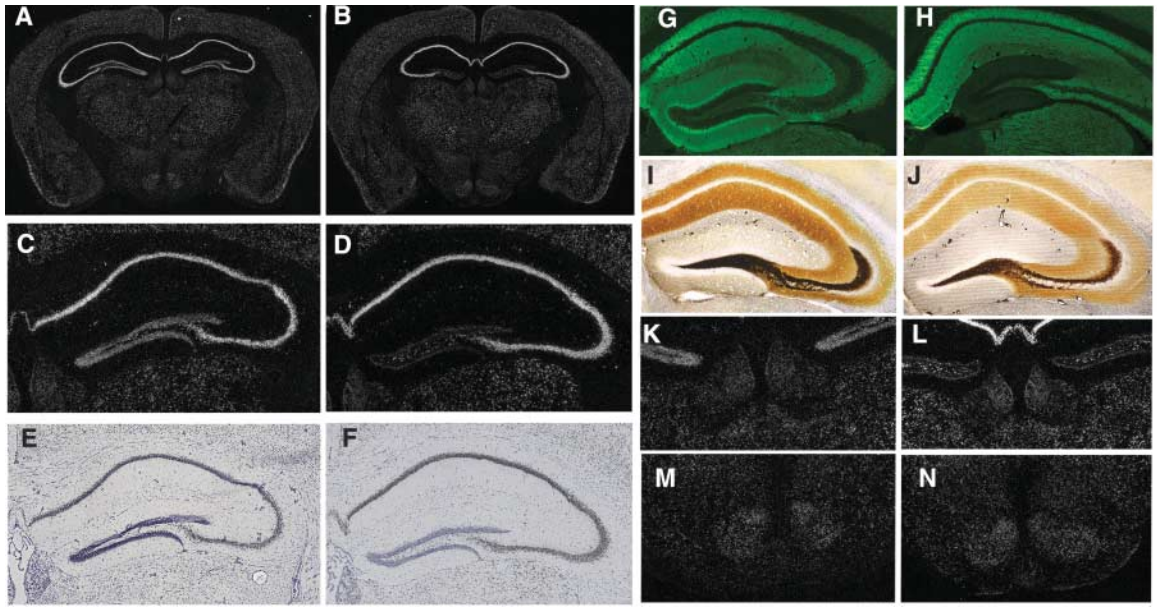

Fig. 2. Basic features of DG-NR1 KO mice. (**A** to **F**) Images of coronal sections after in situ hybridization with a ^{33}P-labeled NR1 cDNA probe. (A) Dark-field image (1× magnification) of a midbrain coronal section from a 20-week-old *f*NR1 control male; (B) 1× image of a midbrain coronal section from a 20-week-old DG-NR1 KO male. (C) Image (4× magnification) of the hippocampus from the control mouse; (D) 4× image of the mutant mouse hippocampus. The NR1 transcript is deleted specifically in the DG granule cell layer in the mutant mouse. Light-field image of (E) the *f*NR1 hippocampus and (F) the DG-NR1 KO hippocampus reveal no changes in the gross structure of the hippocampus. (**G** and **H**) Immunohistochemical labeling of the NR1 protein (visualized with AlexaFlour 488, 4×) in the hippocampus of (G) a *f*NR1 animal at 16-weeks of age and (H) a DG-NR1 KO littermate. There is complete and specific loss of the receptor in the dentate gyrus of the KO mouse. (**I** and **J**) Timms staining of the mossy fiber pathway in (I) a 20-week-old *f*NR1 mouse and (J) a mutant littermate revealed no changes in the structure of the DG outputs as a result of the mutation. (**K** to **N**) In situ hybridization with the NR1 probe did not indicate a reduced NR1 mRNA level elsewhere in the brains of the knockout mice. Examination of 4× dark-field images of (K) the habenular nucleus of a 20-week-old *f*NR1 control animal and (L) a DG-NR1 KO littermate, and (M) the arcuate nucleus of control and (N) DG-NR1 KO mouse, found no difference in the abundance of the transcript in either region in the mutant mice.

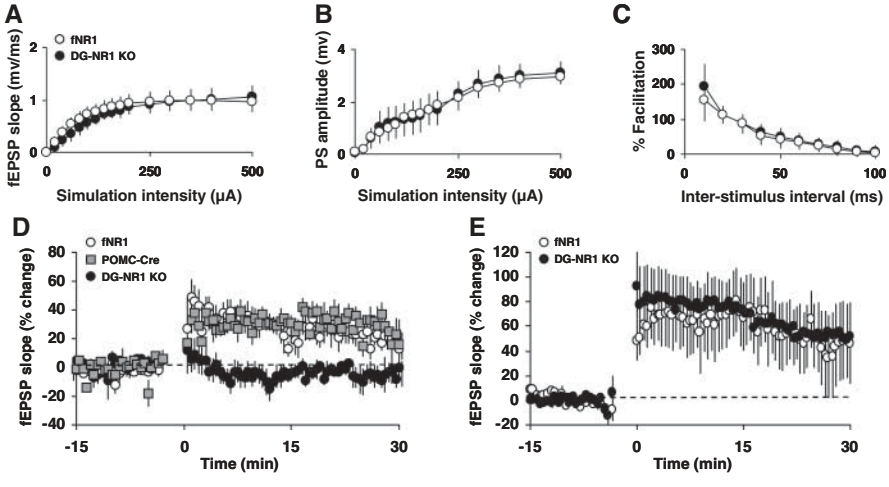

Fig. 3. In vivo synaptic transmission and plasticity of the DG-NR1 KO mice. PP-GC input/output curves of *f*NR1 control (open circles) and mutant (filled circles) mice, showing similar fEPSP slopes (**A**) and population spike (PS) amplitudes (**B**) at all stimulation intensities. (**C**) Paired-pulse facilitation at PP-GC synapses also appeared normal in the mutant mice. (**D**) Theta-burst stimulation of the PP input to the DG induced potentiation of fEPSP in *f*NR1 (open circles) and POMC-cre control animals (squares), but not in DG-NR1 KO mice (filled circles). In contrast, high-frequency stimulation of Schaffer commissural input induced (**E**) CA1 LTP in both DG-NR1 KO mice and *f*NR1 controls. Error bars are the SEMs.

We generated DG-NR1 knockout (KO) mice by crossing these POMC-Cre mice with floxed NR1 (*f*NR1) mice (*29*). In situ hybridization showed that NR1 RNA begins to decrease sometime between 1.5 and 4 weeks after birth and is nearly absent by 16 weeks of age in the DG GCs (Fig. 2, A to F, and fig. S1). Immunocytochemistry with antibodies to NR1 (anti-NR1) showed a total absence of DG GC NR1 protein by 16 weeks of age (Fig. 2, G and H), whereas the hippocampal cytoarchitecture appeared normal (Fig. 2, I and J). We were unable to detect any reduction in the levels of NR1 mRNA or protein in CA1 or CA3 pyramidal cells (Fig. 2, C to H, and fig. S1), the arcuate nucleus of the hypothalamus, neocortex, or the habenular nucleus (Fig. 2, K to N). Furthermore, we did not detect any changes in activity, feeding, reproductive, or parental behaviors in our DG-NR1 KO mice, or in body weight under free-feeding or food-restricted conditions (fig. S2).

Perforant path–dentate gyrus synaptic transmission and plasticity. We examined in vivo synaptic transmission and plasticity in the hippocampus of anesthetized DG-NR1 KO mice and control littermates of 20 to 24 weeks of age. When we stimulated the perforant path (PP) and recorded population responses in the dentate hilus, we found no differences between input-output curves in DG-NR1 KO mice (n = 5) and *f*NR1 littermate controls (n = 4) (Fig. 3, A and B). Paired-pulse facilitation—an index of presynaptic function—also appeared normal in the mutant mice (Fig. 3C). Theta-burst stimulation of the PP evoked robust potentiation of the PP-GC synapses as measured by an increase in the slope of the field excitatory postsynaptic potential (fEPSP) in both the POMC-Cre control mice (n = 3; 30 ± 8.1%) and the *f*NR1 control mice (n = 4; 38 ± 7.7%, P = 0.008) (Fig. 3D). In contrast, identical protocols failed to evoke plasticity in DG-NR1 KO mice (n = 5; change in fEPSP slope = −2.6 ± 6.6%, P = 0.88; DG-NR1 KO × *f*NR1 littermates, P = 0.004) (Fig. 3D). Long-term potentiation (LTP) in area CA1 after high-frequency stimulation of the CA3 Schaffer commissural inputs was normal (*f*NR1: 66 ±

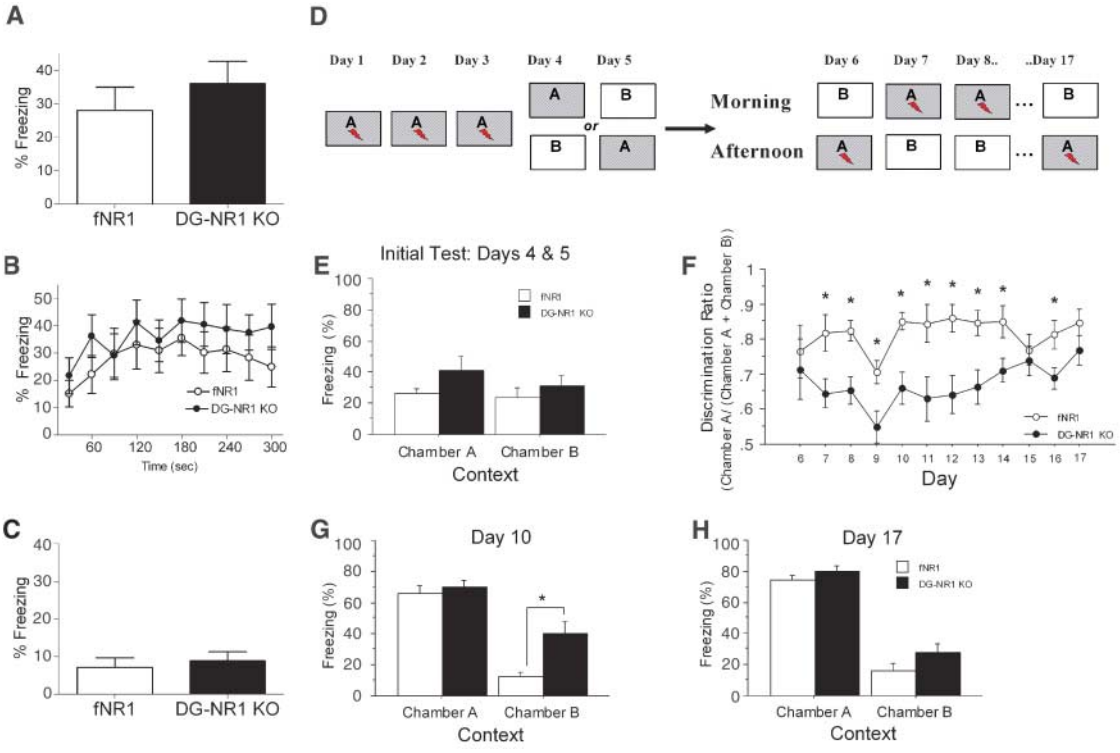

Fig. 4. DG NRs are important for the discrimination of similar contexts. (**A** and **B**) Contextual fear was measured 48 hours after conditioning with a single 2-s 0.75-mA footshock. Both *f*NR1 mice (n = 12) and DG-NR1 KO littermates (n = 12) showed (A) elevated total freezing in the conditioned context, as well as (B) identical kinetics of freezing across the 5-min test. (**C**) Generalized freezing behavior to a second, very different context was low in both genotypes. Separate groups of mice were subjected to a protocol (**D**) designed to test contextual discrimination. For the first 3 days of conditioning, mice visited only chamber A and each day received a single footshock (2 s, 0.65 mA). Freezing was measured once in chamber A and once in chamber B over the subsequent 2 days, and (**E**) control and mutant mice displayed equal amounts of freezing in both chambers. During days 6 to 17, mice visited each chamber daily (receiving a shock in one of the two), and freezing was assessed during the first 3 min in each chamber. (**F**) *f*NR1 mice (open circles; n = 12) showed significantly greater discrimination than the DG-NR1 KO mice (filled circles; n = 12) across most of the acquisition. (**G** and **H**) Freezing in chamber A and chamber B for the control (open bars) and mutant (filled bars) on (G) day 10 (middle of discrimination) and (H) day 17 (end of discrimination) demonstrated that the initial DG-NR1 KO discrimination deficit was rescued with additional training. Error bars in (B) to (H) are the SEMs.

Table 1. Basic properties of pyramidal cells recorded in CA1 and CA3 during exploration of the white circular arena (run 1) on the first day of the pattern separation experiment. Values are means ± SEM. *N*, number of mice; *n*, number of cells.

Measurement	CA1		CA3	
	*f*NR1 (*N* = 5, *n* = 32)	DG-NR1 KO (*N* = 5, *n* = 46)	*f*NR1 (*N* = 5, *n* = 26)	DG-NR1 KO (*N* = 6, *n* = 26)
Mean firing rate (Hz)	0.384 ± 0.047	0.728 ± 0.149	0.378 ± 0.069	0.322 ± 0.049
Spike width (μS)	598 ± 7.65	560 ± 24.8	554.2 ± 12.8	530.5 ± 31.9
Complex spike index (bursting)	18.26 ± 1.76	20.37 ± 1.62	20.29 ± 2.20	22.05 ± 1.96
Peak rate (Hz)	20.53 ± 1.25	18.08 ± 1.37	12.58 ± 1.85	13.07 ± 1.20
Field size (% of sampled space)	24.68 ± 1.78	31.8 ± 2.63*	28.14 ± 3.02	35.9 ± 3.19

*Significantly different from *f*NR1 control (Student's t test, $P < 0.05$).

25%, P = 0.04; DG-NR1 KO: 88 ± 21%, P = 0.04) (Fig. 3E).

Hippocampal memory and discrimination. We first subjected the DG-NR1 KO and control *f*NR1 littermates to the hidden platform version of the Morris water maze and found no detectable deficit in the mutants with the standard protocol (fig. S3). DG-NR1 KO mice also acquired and retained contextual fear conditioning as efficiently as control littermates after a single context-footshock pairing [mice aged 16 to 24 weeks; *f* NR1 control: 28.1 ± 6.9%; DG-NR1 KO: 36.1 ± 6.6%, P = 0.41; two-way analysis of variance (ANOVA): genotype × minute $F(1,9) = 0.65$, P = 0.52; genotype $F(1,9) = 0.70$, P = 0.41; minute $F(1,9) = 4.0$, $P < 0.001$) (Fig. 4, A and B). We examined the context specificity of the conditioning by assessing "freezing" behavior in a second context in which the chamber floor was changed from a metal grid to smooth plastic and the ambient lighting was changed from white to red (*30*). This distinct context evoked significantly lower levels of freezing (similar in the two genotypes) than the conditioned context (Fig. 4C) (*f* NR1 control: 7.1 ± 2.6%; DG-NR1 KO: 8.9 ± 2.4%; ANOVA, genotype × chamber $F(1,1) = 0.37$, P = 0.55; genotype $F(1,1) = 0.92$, P = 0.34; chamber $F(1,1) = 22.28$, $P < 0.0001$; *f*NR1 conditioned × nonconditioned, $P < 0.05$; DG-NR1 KO conditioned × nonconditioned, $P < 0.001$).

To investigate whether the NRs in the DG GCs play a role in behavioral pattern separation, we subjected the DG-NR1 KO mice to contextual fear conditioning using a less distinct pair of contexts (A and B) that shared an identical metal grid floor (*30*), but had unique odors, roofs, and lighting (*31*). In this protocol, conditioning took place incrementally over several days, allowing the effects of repeated experiences to be investigated (*32*) (Fig. 4D). On the first 3 days of the experiment, the mice were placed only into chamber A where, 192 s after being placed, they received a single footshock. On day 4, the mice of each genotype were divided into two groups, with one group of each genotype visiting chamber A and the other visiting chamber B; no group received a footshock in either chamber, and freezing was assessed. On day 5, each mouse visited the chamber opposite to the one visited on day 4, and freezing in the absence of footshock was assessed again. After this contextual conditioning there were no freezing differences between genotypes in chamber A, confirming the ability of the mutant mice to acquire contextual fear conditioning. However, because of a greater similarity between chamber A and chamber B compared to those used in the experiment of Fig. 2, A to C, there was extensive generalization between contexts in both genotypes [$F(1,20)$ =

0.66, $P = 0.43$] (Fig. 4E). During the subsequent discrimination phase of the task, mice visited the two chambers daily for 12 days (day 6 to day 17), always receiving a footshock 192 s after being placed in chamber A, but never in chamber B. Freezing during the first 3 min in each chamber was used to calculate a daily discrimination ratio (Fig. 4F). Control mice quickly learned to distinguish the chambers; however, the DG-NR1 KO mice exhibited a transient, yet very significant, deficit during the acquisition of the discrimination task [F (1,20) = 15.11, $P < 0.001$) (Fig. 4F). This deficit in the mutant mice was exhibited as elevated freezing in the shock-free chamber B [two-way ANOVA, chamber × genotype interaction $F(1,20) = 8.70$, $P < 0.008$; pairwise comparison of chamber B freezing, $P < 0.05$] (Fig. 4G). In contrast, at no point during the task did the mutant animals demonstrate a deficit in freezing to the context paired with shock (chamber A). By day 17 (the 12th day of the discrimination task), the DG-NR1 KO mice could discriminate the two chambers in a manner indistinguishable from that of control mice [two-way ANOVA, chamber × genotype interaction $F(1,20) = 0.84$, $P = 0.37$] (Fig. 4H).

Hippocampal place cells and contextual discrimination. We used multi-tetrode recordings to monitor hippocampal ensemble activity as DG-NR1 KO mice explored two distinct contexts. Mice foraged for scattered food rewards in an open, white, circular low-walled box for a 10-min habituation session. Twenty-four hours later, CA1 and/or CA3 place cell activities were recorded in the same box for 10 min (run1). Mice were then placed in a small "sleep" box for 20 min while the white circular box was replaced with an open, black, square low-walled box, and then animals returned to this new box for a second 10-min run session (run2). Forty-six CA1 pyramidal cells and 26 CA3 pyramidal cells from six mutant mice (age 16 to 24 weeks) and 32 CA1 pyramidal cells and 26 CA3 pyramidal cells from five *f*NR1 control mice (littermate controls; age 16 to 24 weeks) met our threshold of a 0.2-Hz average firing rate in at least one of the two boxes (*20–22*, *31*) (fig. S4 and table S3). Run1 spike widths, complex spike indices, peak firing rates, and average firing rates were similar across genotypes in both CA1 and CA3 (Table 1). However, DG-NR1 KO mice displayed larger place fields in CA1 ($P < 0.05$). Figure 5A shows example rate maps of 10 CA3 neurons from each of the two genotypes in both recording contexts (see also table S2).

We assayed rate remapping in both CA1 and CA3 by comparing the average firing rates of each unit during exploration of the two boxes using (i) the normalized change in average firing rate between the two boxes (rate difference) and (ii) a ratio of firing rates in the two contexts (rate overlap) (*20–22*). In control mice, the rate difference in the CA3 region (0.352 ± 0.043) was significantly greater than that in the CA1 region (0.238 ± 0.037; Bonferroni post-test, $P < 0.01$). In contrast, DG-NR1 KO mice showed similar rate differences in CA3 and CA1 (0.184 ±.0.022 versus 0.199 ± 0.037, respectively; $P = 0.97$) (table S1 and fig. S6). The mutation had a significant effect on the rate difference, with the values measured in the CA3 of the mutant mice significantly lower than those in the CA3 of the control mice [two-way ANOVA, genotype × region $F(1,1) = 3.52$, $P = 0.06$; genotype $F(1,1) = 9.18$, $P = 0.003$; region $F(1,1) = 2.09$, $P = 0.15$; Bonferroni post-test, *f* NR1 CA1 × DG-NR1 KO CA1, $P > 0.05$; *f* NR1 CA3 × DG-NR1 KO CA3, $P < 0.01$) (Fig. 5B). To assess if these rate differences reflected significant rate remapping, we compared actual rate difference values with rate differences for each region expected if the firing rates in the two boxes were independent of one another (Fig. 5B, red lines). Rate differences were significantly lower than expected under fully independent conditions in both CA1 and CA3 of the mutants (CA1 $Z = 5.44$, $P < 0.001$; CA3 $Z = 3.12$, $P < 0.001$), as well as in CA1 of the controls (CA1 $Z = 2.99$, $P < 0.002$). Only the control CA3 data showed evidence of independent firing rates in the two boxes (CA3 $Z = 0.44$, $P = 0.33$). Figure 5C shows the cumulative probability histogram for the rate overlap in CA3 and CA1 regions. In CA3 of control mice, there was a significant shift of the histogram to the left compared to the CA1 (Mann Whitney U test; $P < 0.04$), indicating a greater proportion of CA3 cells undergoing rate remapping. In the KO mice, the distributions of rate overlap values in both CA1 and the CA3 were significantly shifted to the right of the control CA3 histogram and were similar to that of the control CA1 histogram (control CA3 × mutant CA3, $P < 0.01$; control CA3 × mutant CA1, $P < 0.003$).

Place cells can show context-dependent changes in firing location as well as firing rate ["global remapping" (*20*)]. We therefore compared the locations of CA1 and CA3 place fields

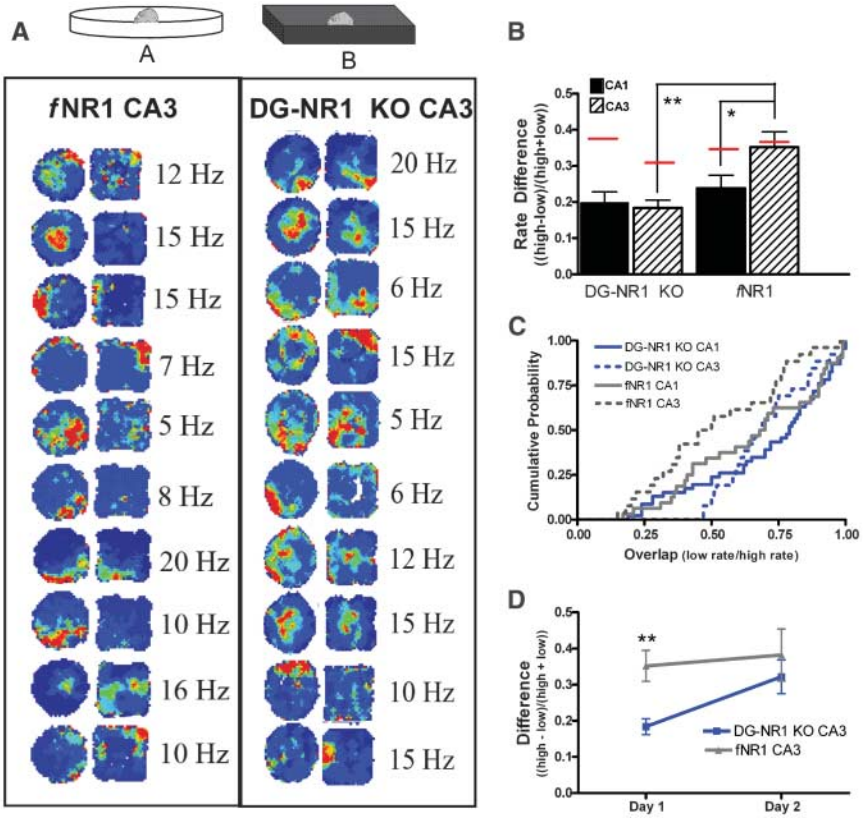

Fig. 5. DG NRs are important for context-specific modulation of firing rate in CA3. (**A**) Examples of firing-rate maps showing the activity of 10 *f*NR1 control (left) and 10 DG-NR1 KO (right) CA3 place cells as mice successively explored a white circular box and a black square box in the same location. Colors are scaled to maximum firing rates given by the numbers (red, maximum; blue, silent). (**B**) The rate difference in average firing rate in the two boxes was calculated for each cell [(high rate − low rate)/(high rate + low rate)]. *f*NR1 control rate differences were larger for CA3 than for CA1, whereas DG-NR1 KO rate differences were similar in CA3 and CA1. Mutant CA3 rate differences were significantly smaller than those of control mice (*$P < 0.05$, **$P < 0.01$). Red lines indicate rate differences expected given independent firing in the two boxes. (**C**) Cumulative probability histograms of the overlap [(low rate)/(high rate)] values for both genotypes and subregions showing significantly greater rate remapping (leftward shift) in control mice. (**D**) When the two box/one room experiment was repeated 24 hours later, DG-NR1 KO also showed significant rate remapping in CA3 (**day 1 $P < 0.01$; day 2 $P = 0.57$). Error bars in (B) and (D) are the SEMs.

in the two contexts by binning averaged firing rates into positional pixels and measuring the distance between peak firing rate pixels in the black and white boxes. Positional remapping was similar across subregions, conditions, and genotypes (mean intercontext shift of 3.0 ± 0.3 and 3.7 ± 0.4 pixels in control CA1 and CA3; 2.7 ± 0.3 and 3.4 ± 0.4 in DG-NR1 KO CA1 and CA3) (SOM Text and fig. S5). Thus, the remapping deficits in DG-NR1 KO mice were confined to the rate remapping dimension under these conditions.

The deficit revealed by the contextual fear discrimination paradigm was limited to the early days of training (Fig. 4, F and G). We therefore investigated whether the deficit in context-mediated firing-rate modulation in the CA3 region of the mutant mice could be overcome with more experience. When the mice were allowed to return to the recording room 24 hours later and the recording protocol was repeated, we found similar rate differences in the CA3 regions of both genotypes (15 CA3 cells in five *f* NR1mice, 0.382 ± 0.072; 20 CA3 cells in four DG-NR1 KO mice, 0.322 ± 0.047; P=0.58). Although we could not detect a significant genotype × day interaction, post-tests revealed that the rate remapping deficit was not present on day 2 in the mutant mice [two-way ANOVA, genotype × day $F(1,1) = 1.45$, $P = 0.23$; genotype $F(1,1) = 6.53$, $P = 0.01$; day $F(1,1) = 3.54$, $P = 0.06$; Bonferroni post-test day1 *f* NR1 × DG-NR KO, $P < 0.01$; day 2 *f* NR1 × DG-NR KO, $P > 0.05$] (Fig. 5D).

Discussion. Using conditional genetic-engineering techniques, we have previously shown that NRs in the CA3 play a crucial role in rapid learning and pattern completion–mediated recall, whereas CA1 NRs are required for the formation of both spatial and nonspatial memory (*9*, *10*, *29*, *33*–*35*). The DG-NR1 KO mice described here allowed us to extend the study to the roles of DG NRs and NR-dependent plasticity. Our data support the notion that DG GC NRs play an important role in rapidly forming a unique memory of a context and discriminating it from similar contexts previously encountered (pattern separation), although they are dispensable for the acquisition of contextual memory per se.

DG-NR1 KO mice exhibited impaired context discrimination early during training in the incremental fear-conditioning paradigm and impaired context-modulated place cell activity in CA3 on the initial day of recording. Both deficits were overcome with training or experience. Together, these data suggest that NR function at PP-GC synapses is important for the animals' ability to discriminate similar contexts rapidly with limited experience, but not for slower acquisition of this ability over more trials. We suggest that common mechanisms underlie the DG-NR1 KO deficits observed at both the behavioral and physiological levels, despite the different timelines of recovery to control levels. These differences may reflect differences between the cues used to define the contexts, the use of conditioning footshocks in the behavioral experiment (*36*), the contribution of non-hippocampal structures in fear conditioning, or the greater sensitivity of the readout in the place cell recordings relative to the behavioral task. The eventual acquisition of the discriminating power by DG-NR1 KO mice may be due to the gradual development of synaptic plasticity at sites downstream of the PP-GC synapses. For example, the recurrent collateral-CA3 synapses may provide a complementary site at which small differences in PP input can be amplified; this is supported by a recent study reporting a contribution of CA3 NRs to pattern separation (*37*). Although the large number of cells and sparse connectivity of the DG would provide the ultimate substrate for the pattern separation, synaptic plasticity may be the tool that allows rapid and efficient separation of representations.

CA3 receives excitatory input from two external sources, the DG and the EC. Input from the DG is most likely to contribute to the orthogonalization of CA3 representations by virtue of the high GC number and the sparse GC-CA3 connectivity. Loss of NRs in the GCs may decrease drive from the DG to CA3. This would increase the relative proportion of EC drive to CA3, thus reducing the CA3 ensemble's ability to detect, amplify, and reflect small differences in EC activity generated in similar contexts. Indeed, rate remapping in CA3 (induced by changes in recording chamber shape or color) can occur in the absence of detectable changes in medial EC firing rates or locations (*25*, *26*). However, despite unvarying input from the EC, DG GCs did respond to contextual changes robustly and rapidly under these conditions. Our data suggest that NR-mediated activity or plasticity in the GCs may underlie these changes, subsequently shaping CA3 encoding.

It is puzzling that rate remapping in CA3 did not always affect spatial or rate coding downstream in CA1 (Fig. 5B) (*20*). It is possible that under different conditions, such as in the behavioral discrimination task, small differences in context-specific coding parameters, including firing rates, could be amplified by contextual salience (such as footshock) and may be manifested in CA1. It remains to be seen whether the context specificity of CA3 coding will be transferred to CA1 under the conditions of behavioral discrimination.

References and Notes

1. W. B. Scoville, B. Milner, *J. Neuropsychiatry Clin. Neurosci.* **12**, 103 (1957).
2. L. E. Jarrard, *Behav. Neural Biol.* **60**, 9 (1993).
3. L. R. Squire, C. E. Stark, R. E. Clark, *Annu. Rev. Neurosci.* **27**, 279 (2004).
4. N. Burgess, E. A. Maguire, J. O'Keefe, *Neuron* **35**, 625 (2002).
5. D. Marr, *Philos. Trans. R. Soc. London B Biol. Sci.* **262**, 23 (1971).
6. J. L. McClelland, N. H. Goddard, *Hippocampus* **6**, 654 (1996).
7. B. L. McNaughton, L. Nadel, in *Neuroscience and Connectionist Theory*, M. A. Gluck, D. E. Rumelhart, Eds. (Erlbaum, Hillsdale, NJ, 1990), pp. 1–63.
8. R. C. O'Reilly, J. L. McClelland, *Hippocampus* **4**, 661 (1994).
9. K. Nakazawa *et al.*, *Science* **297**, 211 (2002).
10. K. Nakazawa *et al.*, *Neuron* **38**, 305 (2003).
11. P. E. Gilbert, R. P. Kesner, *Behav. Brain Res.* **169**, 142 (2006).
12. P. E. Gilbert, R. P. Kesner, I. Lee, *Hippocampus* **11**, 626 (2001).
13. J. O'Keefe, J. Dostrovsky, *Brain Res.* **34**, 171 (1971).
14. S. A. Hollup, S. Molden, J. G. Donnett, M. B. Moser, E. I. Moser, *Eur. J. Neurosci.* **13**, 1197 (2001).
15. K. Louie, M. A. Wilson, *Neuron* **29**, 145 (2001).
16. J. Shen, H. S. Kudrimoti, B. L. McNaughton, C. A. Barnes, *J. Sleep Res.* **7**, 6 (1998).
17. W. E. Skaggs, B. L. McNaughton, *Science* **271**, 1870 (1996).
18. M. A. Wilson, B. L. McNaughton, *Science* **261**, 1055 (1993).
19. I. Lee, D. Yoganarasimha, G. Rao, J. J. Knierim, *Nature* **430**, 456 (2004).
20. S. Leutgeb *et al.*, *Science* **309**, 619 (2005).
21. S. Leutgeb, J. K. Leutgeb, E. I. Moser, M. B. Moser, *Hippocampus* **16**, 765 (2006).
22. S. Leutgeb, J. K. Leutgeb, A. Treves, M. B. Moser, E. I. Moser, *Science* **305**, 1295 (2004).
23. C. Lever, T. Wills, F. Cacucci, N. Burgess, J. O'Keefe, *Nature* **416**, 90 (2002).
24. T. J. Wills, C. Lever, F. Cacucci, N. Burgess, J. O'Keefe, *Science* **308**, 873 (2005).
25. J. K. Leutgeb, S. Leutgeb, M. B. Moser, E. I. Moser, *Science* **315**, 961 (2007).
26. M. Fyhn, T. Hafting, A. Treves, M. B. Moser, E. I. Moser, *Nature* **446**, 190 (2007).
27. N. Balthasar *et al.*, *Neuron* **42**, 983 (2004).
28. P. Soriano, *Nat. Genet.* **21**, 70 (1999).
29. J. Z. Tsien, P. T. Huerta, S. Tonegawa, *Cell* **87**, 1327 (1996).
30. We have shown that the nature of the floor provides a particularly prominent contextual cue.
31. Materials and methods are available as supporting material on *Science* Online.
32. M. S. Fanselow, *Learn. Motiv.* **12**, 398 (1981).
33. P. T. Huerta, L. D. Sun, M. A. Wilson, S. Tonegawa, *Neuron* **25**, 473 (2000).
34. L. Rondi-Reig, M. Libbey, H. Eichenbaum, S. Tonegawa, *Proc. Natl. Acad. Sci. U.S.A.* **98**, 3543 (2001).
35. T. J. McHugh, K. I. Blum, J. Z. Tsien, S. Tonegawa, M. A. Wilson, *Cell* **87**, 1339 (1996).
36. M. A. Moita, S. Rosis, Y. Zhou, J. E. LeDoux, H. T. Blair, *J. Neurosci.* **24**, 7015 (2004).
37. C. J. Cravens, N. Vargas-Pinto, K. M. Christian, K. Nakazawa, *Eur. J. Neurosci.* **24**, 1771 (2006).

38. We thank S. Perry, M. Ragion, C. Lovett, F. Bushard, and L. Leiter for technical assistance. We thank D. Buhl for assistance with the cluster quality measurements and the members of the Tonegawa and Wilson labs for advice and discussion. Supported by National Institute of Mental Health grant MH62122 (M.S.F) and NIH grant P50-MH58880 (S.T.).

Supporting Online Material

www.sciencemag.org/cgi/content/full/1140263/DC1
Materials and Methods
Figs. S1 to S6
Tables S1 to S3
References

23 January 2007; accepted 23 May 2007
Published online 7 June 2007;
10.1126/science.1140263
Include this information when citing this paper.